

Published in final edited form as:

Sci Transl Med. 2011 February 9; 3(69): 69ra12. doi:10.1126/scitranslmed.3001571.

5-Lipoxygenase Metabolite 4-HDHA Is a Mediator of the Antiangiogenic Effect of ω -3 Polyunsaturated Fatty Acids

Przemyslaw Sapielha^{1,2,*}, Andreas Stahl^{1,3,*}, Jing Chen¹, Molly R. Seaward¹, Keirnan L. Willett¹, Nathan M. Krah¹, Roberta J. Dennison¹, Kip M. Connor^{1,†}, Christopher M. Aderman¹, Elvira Liclican⁴, Arianna Carughi^{5,6}, Dalia Perelman^{5,6}, Yoshihide Kanaoka⁷, John Paul SanGiovanni⁸, Karsten Gronert⁴, and Lois E. H. Smith^{1,‡}

¹Department of Ophthalmology, Harvard Medical School, Children's Hospital Boston, 300 Longwood Avenue, Boston, MA 02115, USA

²Department of Ophthalmology, Maisonneuve-Rosemont Hospital Research Centre, University of Montreal, Montreal, Quebec, Canada H1T 2M4

³University Eye Hospital Freiburg, Killianstrasse 5, Freiburg 79106, Germany

⁴Vision Science Program, School of Optometry, University of California, Berkeley, CA 94720, USA

⁵Health Research and Studies Center, Los Altos, CA 94022, USA

⁶Palo Alto Medical Foundation, Palo Alto, CA 94301, USA

⁷Department of Medicine, Harvard Medical School and Brigham and Women's Hospital, Boston, MA 02115, USA

⁸Division of Epidemiology and Clinical Research, National Eye Institute, Bethesda, MD 20892, USA

Abstract

Lipid signaling is dysregulated in many diseases with vascular pathology, including cancer, diabetic retinopathy, retinopathy of prematurity, and age-related macular degeneration. We have previously demonstrated that diets enriched in ω -3 polyunsaturated fatty acids (PUFAs) effectively reduce pathological retinal neovascularization in a mouse model of oxygen-induced retinopathy, in part through metabolic products that suppress microglial-derived tumor necrosis factor- α . To better understand the protective effects of ω -3 PUFAs, we examined the relative

[‡]To whom correspondence should be addressed. lois.smith@childrens.harvard.edu.

*These authors contributed equally to this work.

[†]Present address: Massachusetts Eye and Ear Infirmary, Angiogenesis Laboratory, Department of Ophthalmology, Harvard Medical School, 243 Charles Street, Boston, MA 02114, USA.

Author contributions: P.S., A.S., and L.E.H.S. designed the study, evaluated all data, and wrote the manuscript. P.S. and A.S. participated in all experiments. J.C., J.P.S., and K.G. provided valuable conceptual input. M.R.S., K.L.W., N.M.K., R.J.D., K.M.C., and C.M.A. executed animal work and retinal analyses. K.G. and E.L. performed all lipidomic analyses. A.C. and D.P. recruited patients for human lipidomic experiments. Y.K. generated LTC₄S^{-/-} mice. P.S., A.S., L.E.H.S., J.C., K.G., M.R.S., K.L.W., N.M.K., R.J.D., C.M.A., and E.L. contributed to the total data analysis for preparation of figures. All authors approved the manuscript.

Competing interests: The authors declare that they have no competing interests.

SUPPLEMENTARY MATERIAL

www.sciencetranslationalmedicine.org/cgi/content/full/3/69/69ra12/DC1

Fig. S1. Percentage values for retinal neovascularization quantification.

Fig. S2. Representative images of P17 normoxic retinas from wild-type and 5-LOX^{-/-} mice.

Fig. S3. P17H expression of angiogenic and inflammatory markers from ω -3 PUFA-fed wild types and 5-LOX^{-/-} retinas.

Fig. S4. CAY10606 effect on the formation of the 15-LOX product 17-HDHA.

Fig. S5. Localization and expression of endothelial activation markers ICAM-1 and E-selectin.

importance of major lipid metabolic pathways and their products in contributing to this effect. ω -3 PUFA diets were fed to four lines of mice deficient in each key lipid-processing enzyme (cyclooxygenase 1 or 2, or lipoxygenase 5 or 12/15), retinopathy was induced by oxygen exposure; only loss of 5-lipoxygenase (5-LOX) abrogated the protection against retinopathy of dietary ω -3 PUFAs. This protective effect was due to 5-LOX oxidation of the ω -3 PUFA lipid docosahexaenoic acid to 4-hydroxy-docosahexaenoic acid (4-HDHA). 4-HDHA directly inhibited endothelial cell proliferation and sprouting angiogenesis via peroxisome proliferator-activated receptor γ (PPAR γ), independent of 4-HDHA's anti-inflammatory effects. Our study suggests that ω -3 PUFAs may be profitably used as an alternative or supplement to current anti-vascular endothelial growth factor (VEGF) treatment for proliferative retinopathy and points to the therapeutic potential of ω -3 PUFAs and metabolites in other diseases of vasoproliferation. It also suggests that cyclooxygenase inhibitors such as aspirin and ibuprofen (but not lipoxygenase inhibitors such as zileuton) might be used without losing the beneficial effect of dietary ω -3 PUFA.

INTRODUCTION

Pathological retinal neovascularization is the foremost destructive manifestation of ischemic retinopathies such as diabetic retinopathy (DR) and retinopathy of prematurity (ROP) and a leading cause of blindness worldwide (1–4). Previous work from our group demonstrated that dietary ω -3 polyunsaturated fatty acids (PUFAs) protect against pathologic retinal angiogenesis in a mouse model of oxygen-induced retinopathy (OIR) (5). This result is consistent with recent clinical data showing that decreased ocular neovascularization correlates with increased dietary intake of ω -3 PUFAs (6). Although progress has been made in understanding the protective properties of ω -3 PUFAs (7, 8), we still do not know exactly which lipid-processing pathways and which molecules govern these effects in retinopathy. Deciphering the pathways and bioactive lipid metabolites through which ω -3 PUFAs block angiogenesis in the eye would allow for the development of targeted treatments that may be additive to the currently used anti-VEGF (vascular endothelial growth factor) approaches to treating retinopathy. It would also uncover whether the use of commonly available inhibitors of ω -3 PUFA-related metabolic enzymes that produce bioactive molecules would be counterproductive. These inhibitors include aspirin and nonsteroidal anti-inflammatory drugs (NSAIDs).

The standard explanation for the benefits of ω -3 PUFAs is that eicosapentaenoic acid (EPA) (20:5 ω 3) and DHA (22:6 ω 3) are directly integrated at the sn2 position of membrane phospholipids, resulting in the consequent unseating of structurally similar ω -6 PUFAs, mainly linoleic acid (18:2 ω 6) and arachidonic acid (20:4 ω 6) (9, 10). The relative membrane concentrations of these ω -3 and ω -6 PUFA substrates for phospholipase A₂ (PLA₂) (which catalyzes the hydrolysis of lipids from cell membranes, liberating them for further metabolism) are thought to determine the concentration of downstream proangiogenic or antiangiogenic bioactive metabolites (11). Thus, depending on dietary intake, changes in membrane microdomain composition can shift the substrate pool from ω -6 PUFAs to ω -3 PUFAs, which in turn influences the concentrations of bioactive lipid mediators that are synthesized during the retina's response to stress stimuli (5). To date, this change in lipid membrane composition is thought to exert its effects mainly by modulating the inflammatory state of the tissue: Proinflammatory 2-series prostaglandins and leukotrienes are derived from the ω -6 PUFAs (arachidonic acid), whereas the anti-inflammatory neuroprotectins and D-series resolvins originate from the ω -3 PUFA DHA, and the E-series resolvins and 3-series prostaglandins from EPA (11–13).

The enzymatic pathways that principally process the pool of available ω -3 and ω -6 PUFAs into bioactive metabolites are the cyclooxygenases (COXs) and the lipoxygenases (LOXs) (12) (Fig. 1A). COXs are heme-containing enzymes with peroxidase activity that play a primary role in prostanoid synthesis (10), whereas the LOXs are non-heme iron dioxygenases that insert molecular oxygen with regional specificity into PUFAs (14) and generate isozyme-specific, biologically active products such as the eicosanoid leukotrienes, lipoxins, and the recently identified ω -3 PUFA-derived resolvins and protectins (8, 15). Beneficial effects of dietary ω -3 PUFAs are in part mediated by these COX- and/or LOX-derived autacoids (12).

Given the extensive use of medications such as NSAIDs that inhibit lipid-processing enzymes, it is important to gain a better understanding of the pathways that produce the desirable effects of ω -3 PUFA lipids. Here, we sought to determine the overall contribution of specific COX and LOX enzymatic pathways to the protective effects of ω -3 PUFAs against the destructive neovascularization observed in proliferative retinopathy with the widely used mouse model of OIR that mimics the vasoproliferative phase of ocular neovascular diseases such as ROP and DR. We demonstrated a dominant antiangiogenic role for the 5-LOX pathway and its product 4-hydroxy-docosahexaenoic acid (4-HDHA).

RESULTS

Antiangiogenic effects of ω -3 PUFAs in retinopathy are mediated via the 5-LOX pathway

In a mouse model of OIR on ω -3 or ω -6 PUFA-rich diets, we screened four mouse lines in which specific members of the COX and LOX families (COX-1, COX-2, 5-LOX, and 12/15-LOX) had been knocked out (Fig. 1A). Suppression of pathological neovascularization (Fig. 1B) was assessed at postnatal day 17 (P17) during peak pathological retinal vessel proliferation (16, 17). ω -3 or ω -6 PUFA-rich diets were provided to nursing mouse mothers at delivery. These defined feeds were isocaloric and matched with respect to all nutrients except that the 2% total fatty acid content was either ω -3 (DHA and EPA) or ω -6 (arachidonic acid) PUFAs (5). The lipid composition of mother's milk reflects the lipid content of her diet and is readily transferred to nursing pups (5). Consistent with our earlier findings (5), wild-type mice fed ω -3 PUFA-rich diets show ~50% less retinal neovascularization compared to ω -6 PUFA-fed mice ($P < 0.0001$) (Fig. 1C). We did not use standard rodent chow (normal chow) because it exhibits inconsistencies in the ω -3 and ω -6 PUFA content, even between batches from a single manufacturer (5).

We examined the role of COXs in mediating the beneficial effects of ω -3 PUFAs in mice lacking either constitutive COX-1 or inducible COX-2 and in wild-type littermate controls. Loss of either COX-1 or COX-2 had no effect on the amount of retinal neovascularization in mice fed ω -3 PUFA-rich diets [wild-type versus COX-1^{-/-} or COX-2^{-/-} mice ($P = 0.494$)], indicating that ω -3 PUFAs exerted their antiangiogenic effects independent of either COX enzyme (Fig. 1D). Lack of involvement of COX-2 in the protective effect of ω -3 PUFAs on retinopathy was confirmed in fat-1 mice, which readily convert ω -6 PUFAs to ω -3 PUFAs (18). There was no loss of antiangiogenic effect in fat-1 mice treated with the selective pharmacological inhibitor of COX-2, parecoxib (intraperitoneal injection; 10 mg/kg per day) (fig. S1D). These findings exclude the involvement of COX pathways as major mediators of the direct protective effects of ω -3 PUFAs against retinopathy.

We next investigated the participation in the antiangiogenic effects of ω -3 PUFAs of specific LOXs that form ω -3 PUFA-derived autacoids, leukotrienes, and/or lipoxins, namely, 5-LOX (Alox5) and 12/15-LOX (Alox15) (8, 12, 15, 19). Similar to COX knockout mice, ω -3 PUFA-fed 12/15-LOX knockout mice had similar levels of retinal neovascularization as their matched wild-type controls ($P = 0.4428$) (Fig. 1D), suggesting

that this pathway is not essential for mediating the antiangiogenic effects of dietary ω -3 PUFAs in the retina. In contrast, however, the antiangiogenic effects of ω -3 PUFA diets were completely abolished in 5-LOX knockout mice, where neovascularization areas were 57% greater than in wild-type controls ($P = 0.0071$) (Fig. 1D) and similar to ω -6 PUFA-fed wild-type mice. The amount of retinal neovascularization in 5-LOX knockout mice receiving an ω -6 PUFA diet was not increased over that of ω -3 PUFA-fed 5-LOX knockout mice (Fig. 1E), suggesting that, in retinopathy, 5-LOX primarily generates antiangiogenic ω -3 PUFA metabolites and that proangiogenic 5-LOX metabolites derived from an ω -6 PUFA (arachidonic acid) diet have a smaller effect. No developmental phenotypic vascular differences were detected during normal growth between 5-LOX knockout mice raised in room air and wild-type mice (fig. S2). Together, these observations point to a central role for the 5-LOX pathway in mediating the beneficial effects of ω -3 PUFAs in proliferative retinopathy.

The cysteinyl-leukotriene pathway does not contribute to the protective effects of 5-LOX on retinopathy

5-LOX is responsible for the formation of conjugated triene eicosanoid metabolites with potent biological effects (20). The direct arachidonic acid-derived 5-LOX product is leukotriene A₄ (LTA₄), which is rapidly converted to leukotriene B₄ (LTB₄) by LTA₄ hydrolase (LTA₄H). Alternatively, arachidonic acid is converted to the cysteinyl leukotrienes [slow-reacting substance of anaphylaxis (SRS-A)] LTC₄, LTD₄, and LTE₄ via LTC₄ synthase (LTC₄S) (20), whereas EPA is metabolized to LTC₅, LTD₅, and LTE₅. Peptido-leukotrienes (Fig. 2A) such as the cysteinyl leukotrienes are potential candidate-mediators of vasoproliferation in OIR because they are potent effectors of vascular inflammation and can alter vascular permeability and contractility (21–23).

To determine whether the 5-LOX^{-/-} phenotype observed above was attributable to short circuiting the leukotriene pathway, we investigated the contribution of this pathway to neovascularization in OIR. Given that our lipidomic analysis of retinas on both feeds did not yield appreciable amounts of LTB₄ (<1 pg per retina), we focused on the cysteinyl leukotriene pathway. LTC₄S^{-/-} mice on ω -3 feeds were subjected to OIR, and neovascularization was assessed at P17 as above. In contrast to 5-LOX^{-/-} mice, LTC₄S^{-/-} mice did not show any detectable reduction in the protective effects of ω -3 PUFAs with respect to neovascularization ($P = 0.0929$) (Fig. 2B), suggesting that the protective 5-LOX-derived metabolites are generated upstream of the leukotriene pathway.

VEGF levels remain unaltered in 5-LOX-deficient mice

Of all growth factors involved in vessel growth, VEGF is thought to play a central role in pathological retinal neovascularization (1–4). Given the pronounced increase in destructive retinal neovascularization observed in 5-LOX-deficient mice (Fig. 1D), we determined whether retinal levels of VEGF were higher in 5-LOX^{-/-} mice. Retinal mRNA levels of VEGF assessed by real-time polymerase chain reaction (PCR) revealed no change in expression at P17 of OIR (peak neovascularization) between ω -3 PUFA-fed wild-type and 5-LOX^{-/-} mice ($P = 0.1236$), underscoring that the antiproliferative influence of 5-LOX is not directly VEGF-dependent (Fig. 3). This finding is consistent with the normal retinal vascular development observed in 5-LOX^{-/-} mice (fig. S2) and suggests that approaches to modulate 5-LOX may be complementary to anti-VEGF therapies.

5-LOX is expressed by circulating leukocytes but not retinal cells

The expression of 5-LOX has been thought to be restricted to myeloid cells (20, 24). Nevertheless, given the profound effects of 5-LOX loss on ω -3 PUFA protection in OIR (Fig. 1D), we examined whether this enzyme was expressed by retinal cells. Both PCR (Fig.

4A) and Western blot analysis (Fig. 4B) of phosphate-buffered saline (PBS)–perfused (to remove blood) OIR retinas at P14 revealed that retinal concentrations of 5-LOX were very low, because we were unable to detect retinal expression of 5-LOX mRNA by reverse transcription PCR (RT-PCR). However, concordant with previous reports, 5-LOX mRNA transcript (Fig. 4A) [and protein (~75 kD; Fig. 4B)] was highly expressed in circulating leukocytes isolated from whole blood. These findings agree with the prevailing paradigm that vascular leukocytes provide 5-LOX ω -3 PUFA–derived metabolites to injured or stressed tissues such as the retina during OIR.

DHA-derived 5-LOX metabolites are present in the OIR retina

To identify the 5-LOX ω -3 PUFA–derived metabolite(s) originating from blood leukocytes that conferred the retina protective effect, we performed lipid mediator analysis using liquid chromatography–tandem mass spectrometry (LC/MS/MS)–based lipidomics on serum and retinas (25–28) from ω -3 PUFA–fed mice. In our analysis, we specifically focused on DHA-derived metabolites because DHA is a prominent structural fatty acid present at high concentrations in retina (10) and brain (29) and accounts for up to 1.3% of free fatty acids in serum (30). In contrast, the ω -3 PUFA EPA does not accumulate in appreciable amounts, because it is readily converted to DHA (10) in situ. As LOX isozymes selectively catalyze oxidation of PUFAs by stereoselective and specific enzymatic insertion of molecular oxygen, we investigated the production of two primary and specific 5-LOX–derived DHA products, 4-HDHA and 7-HDHA, in OIR (Fig. 4C).

Given the expression of 5-LOX in leukocytes (Fig. 4, A and B), we investigated in human blood from 28 healthy human patients the relative amounts of 4-HDHA and 7-HDHA generated by leukocytes physiologically activated with blood clotting. The serum concentration of 4-HDHA was more than 20 times that of 7-HDHA [4-HDHA (8.63 ± 1.10 ng/ml) versus 7-HDHA (0.39 ± 0.04 ng/ml); $P < 0.0001$] (Fig. 4D). This preferential generation of 4-HDHA was also observed, but to a lesser extent, in isolated mouse polymorphonuclear leukocytes (PMNs) activated with calcium ionophore in the presence of exogenous DHA to assess the maximal ability of 5-LOX to generate 4-HDHA and 7-HDHA. Consistent with the data above, activated PMNs (6×10^5 cells) generated 247 ± 28 ng of 4-HDHA and 149 ± 18 ng of 7-HDHA ($P = 0.0197$) compared to 0.08 ± 0.01 and 0.79 ± 0.03 ng, respectively, when DHA was not added (Fig. 4E). Blocking 5-LOX with the potent specific inhibitor CAY10606 reduced the formation of both 4-HDHA and 7-HDHA by ~75%. The specificity of this approach for inhibiting 5-LOX was confirmed by demonstrating that the 15-LOX product 17-HDHA was not affected by treatment with CAY10606 (fig. S4A). No human or mouse LOX other than 5-LOX has been shown to generate significant amounts of 4-HDHA or 7-HDHA, nor have any cytochrome P450 enzymes been identified that catalyze selective generation of 4-HDHA or 7-HDHA. These data thus demonstrate a predominant production of 4-HDHA and 7-HDHA by leukocytes that is both ω -3 PUFA– and 5-LOX–dependent.

We continued by assessing the serum concentrations of 4-HDHA and 7-HDHA in ω -3 PUFA–fed mice subjected to OIR, which showed three times more 4-HDHA ($P = 0.0313$) and 2.3 times more 7-HDHA ($P = 0.1540$) in the systemic circulation than did normoxic controls. This increase was 5-LOX–dependent based on our data showing that the rise was completely abolished in 5-LOX knockout mice (Fig. 4F).

In light of the protective role of 5-LOX in retinopathy (Fig. 1D), we next sought to determine whether systemically generated 5-LOX metabolites would be present in OIR retinas and therefore able to act locally on the formation of neovascularization. We measured 4-HDHA (177 pg per retina) and 7-HDHA (62 pg per retina) in the whole retinas of ω -3 PUFA–fed wild-type animals. Values were significantly higher than in 5-LOX

knockout mice [21 pg per retina for 4-HDHA ($P = 0.0003$) and 20 pg per retina for 7-HDHA ($P = 0.0252$)] (Fig. 4G). 4-HDHA was also detected in retinas from room air-raised ω -3 PUFA-fed wild-type mice (101 pg/ μ l), whereas retinas from 5-LOX knockout animals show significantly lower concentrations ($P = 0.0496$) (fig. S4B). Together, these data demonstrate that 4-HDHA and 7-HDHA in OIR are generated by 5-LOX and that their endogenous formation is selectively increased in the retinas of OIR animals. The fact that we also observed 4-HDHA in 5-LOX knockout mice suggests that there is a low level of 5-LOX-independent production of 4-HDHA, which may contribute to the 4-HDHA baseline concentrations seen in all groups. However, the pronounced increase in 4-HDHA in the ω -3 PUFA-fed OIR groups is not observed in 5-LOX knockout mice (Fig. 4G), providing evidence that the OIR-induced increase in 4-HDHA is mediated by 5-LOX.

4-HDHA is antiangiogenic via PPAR γ and independent of effects on inflammation

Recent studies report that enzymatic oxidation products of DHA, such as 4-HDHA, bind to the nuclear lipid receptor peroxisome proliferator-activated receptor γ (PPAR γ) (26, 31, 32) and provoke PPAR γ activation to levels similar to or greater than those induced by the PPAR γ -selective agonist pioglitazone or the naturally occurring prostaglandin-derived PPAR γ agonist 15d-PGJ2 (33). We therefore explored the propensity of 4-HDHA and 7-HDHA to directly modulate PPAR γ -controlled angiogenesis. In cultured human retinal endothelial cells (HRECs), 4-HDHA induced a 300% increase in PPAR γ mRNA expression measured by real-time PCR ($P = 0.0457$), whereas 7-HDHA was ineffective (Fig. 5A). To investigate further the effects of these DHA derivatives on endothelial cell function, we performed an MTT [3-(4,5-dimethylthiazol-2-yl)-2,5-diphenyltetrazolium bromide] cell proliferation assay in HRECs. After 36 hours of incubation, 4-HDHA (3 μ M) inhibited cell proliferation by 45% ($P < 0.0001$), whereas 7-HDHA (3 μ M) did not significantly affect endothelial cell division ($P = 0.8059$) (Fig. 5B). To determine whether the observed effects were due to activation of PPAR γ , we used the irreversible, selective PPAR γ antagonist GW9662. The antiproliferative effect of 4-HDHA seemed to be mediated via PPAR γ , because treatment with GW9662 completely reversed the inhibition ($P = 0.0017$). These data were corroborated by two independent and complementary assays of sprouting angiogenesis. First, in a spheroid assay of endothelial microvascular cell sprouting (34), 4-HDHA efficiently abrogated spheroidal sprouting by 65% ($P = 0.0046$), whereas 7-HDHA did not significantly reduce spheroidal sprouting ($P = 0.07$) (Fig. 5C). Second, in an aortic explant *ex vivo* model of vascular sprouting (35), 4-HDHA also attenuated vascular sprouting by ~60% ($P = 0.0382$) (Fig. 5D). As in the endothelial proliferation assay results, the antiangiogenic effect of 4-HDHA was dependent on PPAR γ in both the spheroid assay ($P = 0.0046$) (Fig. 5C) and the aortic sprouting assay ($P = 0.0215$) (Fig. 5D) given the ability of GW9662 to reverse the inhibitory effects of 4-HDHA on vascular proliferation. Because each of these experiments was *ex vivo* in isolated endothelial cell monocultures, the antiangiogenic effects of 4-HDHA seen in this context therefore must be independent of inflammation. Together, these data suggest a role for 4-HDHA in directly blocking endothelial cell proliferation and sprouting angiogenesis via the fatty acid receptor PPAR γ .

The protective effects of ω -3 PUFAs in retinopathy are mediated via PPAR γ

We next examined the expression of PPAR γ in retinas of mice receiving either ω -3 or ω -6 PUFA-enriched diets. PPAR γ levels, as detected by Western blotting and quantified by densitometry, were significantly elevated in ω -3 PUFA-fed (versus ω -6 PUFA-fed) mouse retinas throughout the neovascular phase of OIR (Fig. 6A). Laser capture microdissection of normal vessels and pathological OIR vessels followed by quantitative RT-PCR localized PPAR γ to retinal vessels. There was a robust 800% PPAR γ mRNA induction in new pathological vessels isolated by laser capture from ω -3 PUFA-fed P17 OIR retinas compared to pathological vessels isolated from OIR retinas of ω -6 PUFA-fed mice (Fig.

6B). These data, together with the data presented above, form a rationale for exploring the contribution of this receptor to the antiangiogenic effects of ω -3 PUFAs in retinopathy. Indeed, inhibition of PPAR γ by administration of GW9662 [daily intraperitoneal injection (1 mg/kg) from P12 to P17] to wild-type mice receiving ω -3 PUFA diets effectively abrogated the antiangiogenic effects of ω -3 PUFAs as the neovascular area increased from 7.6 to 10.9% ($P = 0.004$), yielding areas of neovascularization akin to those observed in both ω -6 PUFA-fed wild-type mice (11.2%; fig. S1A) and ω -3 PUFA-fed 5-LOX knockout animals (11.3%; Fig. 6C). Collectively, these data support our *in vitro* findings, suggesting a role of PPAR γ in mediating the antiangiogenic effects of ω -3 PUFA metabolites.

DISCUSSION

Although the beneficial effects of ω -3 PUFAs on human health have been reported since the beginning of the last century (36), our knowledge of the primary mechanisms by which these lipids exert their protective effects remains relatively limited. Here, we present two concepts regarding the actions of ω -3 PUFAs as antiangiogenic compounds for proliferative retinopathies. First, we identify 5-LOX (and not COX-1 or COX-2) as the central generator of angiostatic mediators of ω -3 PUFAs in the retina. Second, we find a key role for 5-LOX-derived 4-HDHA in the antiangiogenic effects of ω -3 PUFAs and identify PPAR γ as the receptor governing these effects. In addition, we report significant 4-HDHA concentrations in healthy human subjects, suggesting that our findings may apply to ω -3 PUFA action in humans.

Lipid mediators have been considered as proinflammatory because NSAIDs inhibit prostaglandin and thromboxane synthesis. In this respect, the antiangiogenic properties of 5-LOX and its products may seem counterintuitive. Nevertheless, although 5-LOX can generate potent proinflammatory, ω -6 PUFA (arachidonic acid)-derived products such as leukotrienes (20), in later phases of inflammation, 5-LOX switches to producing anti-inflammatory/pro-resolving ω -6 PUFA-derived lipoxins (37) and ω -3 PUFA-derived resolvins (38). Consistent with this antiinflammatory role of 5-LOX, loss of 5-LOX in knockout retinas is associated with significantly increased levels of inflammatory mediators (fig. S3) and markers of endothelial cell activation (fig. S5). We have previously demonstrated that certain bioactive ω -3 PUFA derivatives [notably the 5-LOX-derived resolvin E1 (RvE1)] protect against retinal neovascularization (5). These beneficial effects are thought to occur in part via inhibition of tumor necrosis factor- α (TNF- α) derived from microglia in the retina, confirming that suppression of inflammation with antiinflammatory mediators such as RvE1 can suppress pathological neovascularization (5). The findings presented in this study are complementary to this earlier work in that they describe an additional directly antiangiogenic, 5-LOX-derived ω -3 metabolite, 4-HDHA. The effect of 5-LOX-derived 4-HDHA is independent of the previously established antiinflammatory effects of resolvin-related 5-LOX metabolites because 4-HDHA has potent effects in endothelial cell sprouting assays in which no immune cells are present to modulate inflammation. Together, these results confirm a central role for 5-LOX in generating direct ω -3-derived antiangiogenic mediators that act both through anti-inflammatory pathways and directly to inhibit endothelial cell proliferation and sprouting angiogenesis independent of alterations in inflammatory activation.

5-LOX is an obligatory enzyme for the formation of LTB₄ and peptido-leukotrienes, which are important in inflammation and potentially in angiogenic responses in tumors (24). However, our lipidomic analysis did not detect LTB₄ or peptido-leukotriene precursors in the retina. Moreover, deletion of the essential enzyme for generating peptido-leukotrienes (LTC₄S) did not affect pathological retinal neovascularization in wild-type mice on ω -3 PUFA diets. These findings eliminate leukotrienes as major modulators of OIR-induced

angiogenesis. Although other ω -3 PUFA derivatives such as NPD1 (a direct 12/15-LOX DHA-derived product) have potent anti-inflammatory and neuroprotective properties (15, 39, 40), the 12/15-LOX pathway was not essential for mediating the antiangiogenic action of dietary ω -3 PUFAs. Although complementary pathways might contribute to generating NPD1 and other bioactive molecules involved in resolving inflammation, our data implicate direct metabolism of DHA by 5-LOX as the major source of ω -3-derived antiangiogenic signals in the retina.

In addition, we identify PPAR γ as a receptor for mediating the antiangiogenic properties of ω -3 PUFAs. PPAR γ is also the high-affinity receptor for the insulin-sensitizing and antidiabetic thiazolidinediones (41, 42) such as the Food and Drug Administration (FDA)-approved rosiglitazone and pioglitazone. Similar to 5-LOX-derived ω -3 PUFA metabolites, these pharmacological agonists prevent pathological retinal neovascularization in a mouse model of OIR (43) and reduce proliferative retinopathy in human diabetic patients (44). Rosiglitazone, although useful for lowering blood sugar, may increase the risk of heart disease in diabetic patients (45), whereas ω -3 PUFAs lower the risk of cardiovascular disease (46) and thus may be a potential alternative to currently marketed PPAR γ agonists. Future clinical studies are required to establish the therapeutic merits of ω -3 PUFA supplementation as an alternative or adjunctive therapy to currently used insulin-sensitizing and antidiabetic PPAR γ agonists in humans.

Establishing the contribution of the major COX and LOX pathways to the generation of beneficial ω -3 PUFA metabolites is important from a translational perspective because these enzymes are the targets of common over-the-counter medications such as aspirin and other NSAIDs (for example, ibuprofen) or of prescription medications such as zileuton and celecoxib, which are used to treat asthma and arthritis, respectively.

This study reports an *in vivo* assessment of the relative contribution of the major ω -3 and ω -6 PUFA-metabolizing pathways to the modulation of pathological angiogenesis in the mouse model of OIR (47). This model serves as a proxy for human ocular neovascular diseases such as ROP and DR characterized by a late phase of destructive pathological angiogenesis (2). Studies using this model (48, 49) have been translated to treatment for neovascular age-related macular degeneration (AMD) (50). Although the secondary pathological neovascularization observed in this model shares many biochemical similarities to the neovascular phase of human retinopathy (51), the model is not identical to human disease. The avascular area of the retina is more central in the mouse model than the more peripheral avascular area in human ROP. The etiology of vessel loss in the model (hyperoxia) differs from the hyperglycemia-induced damage observed in DR. However, the model can be used to address the molecular mechanisms by which dietary ω -3 PUFAs influence ocular neovascularization to give direction to clinical trials.

In line with the central role for 5-LOX, the protective effects of ω -3 PUFAs persist in COX-1 and COX-2 knockout mice, as well as in mice receiving the COX-2 inhibitor parecoxib. These results suggest that the widely used COX inhibitors will not block the beneficial effects of ω -3 PUFAs. Aspirin triggers production of a newly identified family of 5-LOX-dependent anti-inflammatory lipids, the aspirin-triggered lipoxins (ATLs) (19, 52, 53). The aspirin-acetylated COX-2 catalytic site remains active and readily produces substrates that are later converted into ATLs by 5-LOX. Moreover, COX-2 modified by aspirin metabolizes EPA and DHA into bioactive epimers of resolvins (RvE1 and RvDs) and protectins (52, 54, 55) and would be expected to potentially further attenuate retinal neovascularization (5). The production of antiangiogenic/pro-resolving lipids via the cooperative action of COX and 5-LOX circuits suggests that future therapeutic interventions may be specifically tailored to maximize production of these protective metabolites. Clinical

use of 5-LOX inhibitors, such as the FDA-approved drug zileuton, in patients at risk of ocular neovascular disease warrants closer investigation in light of our findings that 5-LOX is central to the production of antiangiogenic metabolites. In contrast, aspirin or NSAID use in patients would not be expected to negate the benefits of an ω -3 PUFA-rich diet.

As current therapies for proliferative retinopathies are largely restricted to invasive interventions such as laser photocoagulation or intraocular injections, there is presently a need for safe, efficient, and readily available treatments. The cost of intervention with ω -3 PUFAs is very low (~\$10 per month) compared to the cost of intraocular injections of anti-VEGF treatment, which is up to \$4000 per month. Dietary intervention with ω -3 PUFAs may be an attractive, easily applicable, and cost-effective strategy that could provide an adjunct to current regimes such as intraocular injections of anti-VEGF drugs. There is an ongoing multicenter Phase 3 randomized clinical trial (AREDS2) designed to assess the effects of oral supplementation of ω -3 PUFAs as a treatment for AMD. The use of NSAIDs and aspirin will also be assessed. Similar clinical trials are needed to evaluate ω -3 PUFAs and COX and LOX enzyme inhibitors in ROP and DR.

Our data also identify a direct antiangiogenic role for ω -3 PUFA-derived and 5-LOX-metabolized 4-HDHA. These findings can serve as the foundation for exploring new treatment regimes tailored for prevention of ocular neovascularization, as well as for possible treatment of systemic diseases with perturbed vascular growth such as cancer.

MATERIALS AND METHODS

Animals

All studies adhered to the Association for Research in Vision and Ophthalmology Statement for the Use of Animals in Ophthalmic and Vision Research and were approved by the Children's Hospital Boston Animal Care and Use Committee. C57BL/6 wild-type (WT), 5-LOX^{-/-}, and 12/15-LOX^{-/-} mice were purchased from Jackson Laboratories. COX-1^{-/-} (Taconic strain 002180-M and WT control 002180-W) and COX-2^{-/-} (COX-2 Taconic strain 002181-M and WT control 002181-W) were from Taconic Farms. LTC₄S^{-/-} mice were generated as described (56) and backcrossed on C57BL/6 backgrounds for more than 10 generations. *fat-1* mice were generated as described (18). All mice were weighed at the end of experiments, and mice less than 5 g at P17 were not included in data analysis (16).

O₂-induced retinopathy

Mice were exposed to 75% oxygen from P7 to P12. Upon return to room air, hypoxia-driven neovascularization is initiated and forms from P14 onward until peak neovascularization is reached on P17 (16, 47). Retinal neovascularization was evaluated at the disease peak (P17) as described. Briefly, mice were given a lethal dose of avertin (Sigma-Aldrich), and eyes were enucleated and fixed in 4% paraformaldehyde for 1 hour at room temperature. Retinas were dissected and stained overnight at room temperature with fluoresceinated Isolectin B4 (Alexa Fluor 594, I21413, Molecular Probes) in 1 mM CaCl₂ in PBS. Lectin-stained retinas were whole-mounted onto Superfrost/Plus microscope slides (Fisher Scientific) with the photoreceptor side down and imbedded in SlowFade Antifade reagent (Invitrogen). For quantification of retinal neovascularization, 20 images of each whole-mounted retina were obtained at 5 \times magnification on a Zeiss AxioObserver.Z1 microscope and merged to form one image with AxioVision 4.6.3.0 software. Neovascularization was analyzed with the SWIFT_NV method (17).

ω -3 and ω -6 PUFA diets

Mouse mothers with pups were fed from birth with defined rodent diets with 10% (w/w) safflower oil containing either 2% ω -3 PUFAs (DHA and EPA) for the treatment group or 2% ω -6 PUFAs (arachidonic acid) for the control group. Both diets have been described in detail (5). The lipid composition of the mother's milk reflects the mother's diet (57,58), and changes in the mother's are efficiently transferred to the pups (5). Dietary PUFAs were produced by DSM Nutritional Products under the trade name ROPUFA. The arachidonic acid and DHA supplements, under the trade names ARASCO and DHASCO, respectively, were obtained from Martek Biosciences Corp. The feed was produced at Research Diets Inc. The composition of this diet has been previously described, and lipids in the diet are stable over time with respect to oxygen exposure over the course of the experiments and with cold storage of feed for a year (5). Standard rodent chow ("normal feed") as a control diet is not suitable because oil composition in rodent chow varies from batch to batch and is not specified by the manufacturer.

Pharmacological inhibition of PPAR γ or COX-2

The irreversible PPAR γ inhibitor GW9662 (2-chloro-5-nitrobenzanilide, Cayman Chemical), a specific antagonist with a nanomolar inhibitory concentration (59) that has been shown to effectively block PPAR γ in vivo (60), was injected intraperitoneally once daily in a concentration of 1 mg/kg in 20 μ l of total volume from P14 to P17. GW9662 was identified in a competition-binding assay against the human PPAR γ ligandbinding domain (region E/F). Controls were injected with vehicle [PBS/DMSO (dimethyl sulfoxide), 1:1] only. Alternatively, parecoxib (Dynastat; Pfizer) was injected intraperitoneally at 10 mg/kg per day.

RT-PCR and quantitative real-time PCR analysis

Eyes were rapidly enucleated and whole retinas (or laser-captured neovessels) were processed for RNA, followed by treatment with de-oxyribonuclease (DNase) I (Qiagen) to remove any contaminating genomic DNA. The DNase-treated RNA was then converted into complementary DNA (cDNA) with reverse transcriptase (Invitrogen). PCR primers targeting TNF- α , interleukin-1 β (IL-1 β), IL-6, IL-10, intercellular adhesion molecule-1 (ICAM-1), E-selectin, VEGF, and the control gene cyclophilin A were designed with Primer Bank and National Center for Biotechnology Information (NCBI) Primer Blast software. Quantitative analysis of gene expression was generated with an ABI Prism 7700 Sequence Detection System and the SYBR Green Master Mix kit, and gene expression was calculated relative to cyclophilin A expression with the ΔC_T method.

Western blotting

Retinal samples were obtained as described above. Pooled retinal lysate (30 μ g) from three different animals was loaded on an SDS-polyacrylamide gel electrophoresis (SDS-PAGE) gel and electroblotted onto a poly-vinylidene difluoride (PVDF) membrane. White blood cells were isolated with a red blood cell (RBC) lysis buffer (Sigma-Aldrich), and 30 μ g of protein was loaded. After blocking, the membranes were incubated overnight with 1:500 rabbit antibody to mouse 5-LOX (C49G1; Cell Signaling) or 1:500 rabbit antibody to mouse PPAR γ (N-20, sc1884; Santa Cruz Biotechnology). After washing, membranes were incubated with 1:2000 horseradish peroxidase-conjugated anti-rabbit secondary antibody (Amersham) for 1 hour at room temperature. Densitometry measurements of immunoreactive bands were carried out with the ImageJ software.

Lipid mediator lipidomics

For endogenous lipid autacid analysis, frozen retinas were homogenized with a handheld tissue grinder in 66% methanol (4°C). Serum samples (20 to 200 µl) were combined with two volumes of methanol (4°C, 40 to 400 µl). The methanol contained deuterated internal standards, prostaglandin E2 (PGE₂-d₄), 15(*S*)-hydroxyeicosatetraenoic acid [15(*S*)-HETE-d₈], and LTB₄-d₄ (400 pg each), to calculate the recovery of different classes of oxygenated fatty acids. Lipid autacoids were extracted by solid phase with Accubond ODS-C18 cartridges (Agilent Technologies) (61). Eicosanoids and docosanoids were identified and quantified by LC/MS/MS-based lipidomics (25–28). In brief, we analyzed extracted samples by a triple-quadruple linear ion trap LC/MS/MS system (MDS SCIEX 3200 QTRAP) equipped with a LUNA C18-2 mini-bore column, using a mobile phase (methanol/water/acetate, 65:35:0.02, v/v/v) with a 0.5 ml/min flow rate. MS/MS analyses were carried out in negative ion mode, and hydroxy fatty acid was quantified by multiple reaction monitoring (MRM) mode with established transitions for eicosanoids and docosanoids, which included 343→101 mass/charge ratio (*m/z*) for 4-HDHA and 343→113 *m/z* for 7-HDHA (25, 27, 28, 32). Calibration curves (1 to 1000 pg) and specific LC retention times for each compound were established with synthetic standards (Cayman Chemical). Structures were confirmed for selected samples by MS/MS analyses with enhanced product ion mode with appropriate selection of the parent ion in quadrupole 1.

Collection and analysis of human serum samples

Healthy male subjects were enrolled as part of a dietary study by the Health Research and Studies Center Inc., and the study was approved by the External Review Board, a compensated and independent Nutrition Research Review Committee composed of health professionals (San Francisco, CA). The approved protocol for collecting serum and informed consent comports with the California Health and Safety Code, Section 24170 at Chapter 1.3 regarding a human subject's right to know. The following inclusion criteria were used: males aged 35 to 65 years, a fasting blood glucose level at screening of <110 mg/dl, and body mass index (BMI) <30 and >18.5 kg/m². The subjects were interviewed by a nutritionist and had to complete a prospective diet diary. The following exclusion criteria were used: taking regular fish oil or ω-3 PUFA supplements; eating fish more frequently than once a week; diagnosis of diabetes, kidney, or liver disease, asthma, or acute illness; and use of corticosteroids, NSAIDs, or immunosuppressants. The demographics (mean ± SD) for the 28 male subjects were age 50.3 ± 7.1 years, BMI of 24.5 ± 3.2 kg/m², and blood pressure of 119.2 ± 12.5/75.7 ± 9.0 mmHg (systolic/diastolic). Fasting blood samples were collected in the evening to establish basal levels of serum fatty acids. Blood was collected from the antecubital fossa vein with venipuncture, and blood was allowed to spontaneously clot. Serum was collected and snap-frozen for solidphase extraction and LC/MS/MS-based lipidomic analysis.

PMN metabolism of DHA

C57BL/6J stock 000664 mice (6 to 10 weeks old; Jackson Laboratory) were injected intraperitoneally with 1 mg of zymosan A (Sigma) in 1 ml of sterile saline [Hanks' balanced salt solution (HBSS), pH 7.4]. Mice were anesthetized subcutaneously with Ketaset (ketamine, 50 mg/kg) and xylazine (20 mg/kg) 16 hours after zymosan A injection, and PMNs were collected by peritoneal lavage (5 ml of sterile HBSS). PMN counts were performed by microscopy with a hemocytometer. The peritoneal exudates were briefly centrifuged, and PMNs were resuspended in serum-free basal medium-2 (600,000 cells per 0.5 ml of medium; Lonza Walkersville Inc.). PMNs were incubated at 37°C for 15 min with 2 µM Ca²⁺ ionophore (A23187; Fisher Scientific) alone or for 5 min with 10 µM DHA (Cayman Chemical) followed by 10 min of 2 µM Ca²⁺ ionophore in the presence or absence of a specific 5-LOX inhibitor (CAY10606, 50 µM, Cayman Chemical). Enzymatic reactions

were terminated through the addition of 2× volume methanol. Samples were then processed for lipidomic analyses to quantify the formation of 5-LOX-specific DHA metabolites (4-HDHA and 7-HDHA) and a 15-LOX-specific DHA metabolite (17-HDHA). DHA-derived products were quantified by MS/MS-based lipidomic analyses with a triple-quadrupole linear ion trap LC/MS/MS system and multiple reaction monitoring with specific and established transition ions.

Laser capture microdissection

Eyes with OIR or normoxic controls were enucleated at P14 and embedded in optimal cutting temperature (OCT) compound. The eyes were sectioned at 12 μm in a cryostat, mounted on ribonuclease (RNase)-free polyethylene naphthalate glass slides (11505189, Leica), and immediately stored at -80°C. Slides containing frozen sections were fixed in 50% ethanol for 15 s, followed by 30 s in 75% ethanol, before being washed with diethyl pyrocarbonate (DEPC)-treated water for 15 s. Sections were stained with fluoresceinated Isolectin B4 (Alexa Fluor 594, I21413, 1:50 dilution in 1 mM CaCl₂ in PBS) and treated with RNase inhibitor (03 335 399 001, Roche) at 25°C for 3 min. Neovessels were laser-microdissected with the Leica LMD 6000 system (Leica Microsystems) and collected directly into lysis buffer from the RNeasy Micro kit (Qiagen).

MTT proliferation assay

HRECs were obtained from Cell Systems and used from passage 2 to 7. Cell number was determined with the MTT assay as described (62). 4-HDHA (3 μM), 7-HDHA (3 μM), and GW9662 (3 μM) were introduced to medium upon seeding, and cell viability was assessed 36 hours after.

Spheroidal sprouting angiogenesis

HRECs were used from passage 2 to 7 for sprouting experiments. Cells were cultured as monolayers at 37°C and 5% CO₂ in a humidified atmosphere in complete medium (Cell Systems). The preparation of endo-thelial cell spheroids was performed as described (34, 63). Briefly, cells were harvested from subconfluent monolayers by trypsinization and suspended in complete medium containing 10% fetal bovine serum (FBS) and 0.25% (w/v) carboxymethylcellulose (Sigma). Five hundred cells were seeded together in one hanging drop to assemble into a single spheroid within 24 hours at 37°C and 5% CO₂. After 24 hours, spheroids were harvested and used for sprouting analysis in a matrix of type I collagen. Briefly, 30 endothelial cell spheroids per group were seeded into 0.5 ml of collagen solution in nonadherent 24-well plates, with a final concentration of rat type I collagen of 1.5 mg/ml. Freshly prepared gels were transferred rapidly into a humidified incubator (37°C, 5% CO₂), and after the gels had solidified, 0.1 ml of serum-free medium (Cell Systems) was added per well containing DHA derivatives and/or PPARγ inhibitors as indicated. After 24 hours, gels were photographed and spheroid sprouting was assessed quantitatively with Adobe Photoshop. Results are expressed as means ± SEM.

Microvascular sprouting from aortic explants

Aortae from C57BL/6 WT mice were cut into 1-mm-thick rings and placed in growth factor-reduced Matrigel (BD Biosciences) in 24-well tissue culture plates and cultured for 4 days in EBM-2 medium (Clonetics) (35). 4-HDHA (3 μM), 7-HDHA (3 μM), and GW9662 (3 μM) were introduced to the culture medium 48 hours and then 72 hours after seeding. Photomicrographs of individual explants were taken 96 hours after plating (48 hours after treatment), and microvascular sprouting was quantified by measuring the area covered by outgrowth of the aortic ring with Adobe Photoshop. Results are expressed as means ± SEM.

Immunohistochemistry

For immunohistochemistry, eyes were enucleated from mice and fixed in 4% paraformaldehyde at room temperature for 1 hour. The retina was isolated, permeabilized overnight at 4°C with 0.1% Triton X-100 (T-8787, Sigma) in PBS, and stained with fluoresceinated Isolectin B4 (Alexa Fluor 594, I21413) in 1 mM CaCl₂ in PBS for retinal vasculature. Antibodies to ICAM-1 (AF796, R&D Systems) and E-selectin (ab2497, Abcam) were used for localization studies according to the manufacturers' recommendations. Flat mounts were visualized with 40× objectives on a Zeiss AxioObserver.Z1 microscope, and images were obtained with a Zeiss AxioCam MRm and AxioVision 4.6.3.0. software.

Statistical analysis

Results are presented as means ± SEM for all animal studies and means ± SD for all other studies. Analysis of variance with significance $\alpha = 0.05$ was used for processing all data. Two-tailed *t* tests were used to test for significance.

Supplementary Material

Refer to Web version on PubMed Central for supplementary material.

Acknowledgments

We thank B. Dong and A. Sullivan for running the LC/MS/MS-based lipidomic analyses.

Funding:

This work was supported by NIH grants EY017017, EY017017-04S1 (L.E.H.S.), and EY016136 (K.G.); Children's Hospital Boston Mental Retardation and Developmental Disabilities Research Center grant P01 HD18655 (L.E.H.S.); Research to Prevent Blindness Senior Investigator Award (L.E.H.S.); Alcon Research Institute Award (L.E.H.S.); MacTel Foundation (L.E.H.S.); Roche Foundation for Anemia Research (L.E.H.S.); and V. Kann Rasmussen Foundation (L.E.H.S.). P.S. holds a Canada Research Chair in Retinal Cell Biology and is supported by grants from the Canadian Institutes of Health Research, the Charles A. King Trust Award, and the Canadian National Institute for the Blind. A.S. is funded by Deutsche Forschungsgemeinschaft. Additional support was provided by the Juvenile Diabetes Research Foundation International (J.C.), the William Randolph Hearst Award F32 EY017789 (K.M.C.).

REFERENCES AND NOTES

- Chen J, Smith L. Retinopathy of prematurity. *Angiogenesis*. 2007; 10:133–140. [PubMed: 17332988]
- Sapieha P, Hamel D, Shao Z, Rivera JC, Zaniolo K, Joyal JS, Chemtob S. Proliferative retinopathies: Angiogenesis that blinds. *Int. J. Biochem. Cell Biol.* 2010; 42:5–12. [PubMed: 19836461]
- Sapieha P, Joyal JS, Rivera JC, Kermorvant-Duchemin E, Sennlaub F, Hardy P, Lachapelle P, Chemtob S. Retinopathy of prematurity: Understanding ischemic retinal vasculopathies at an extreme of life. *J. Clin. Invest.* 2010; 120:3022–3032. [PubMed: 20811158]
- Smith LE. Pathogenesis of retinopathy of prematurity. *Semin. Neonatol.* 2003; 8:469–473. [PubMed: 15001119]
- Connor KM, SanGiovanni JP, Lofqvist C, Aderman CM, Chen J, Higuchi A, Hong S, Pravda EA, Majchrzak S, Carper D, Hellstrom A, Kang JX, Chew EY, Salem CN Jr, Serhan CN, Smith LE. Increased dietary intake of ω -3-polyunsaturated fatty acids reduces pathological retinal angiogenesis. *Nat. Med.* 2007; 13:868–873. [PubMed: 17589522]
- SanGiovanni JP, Chew EY, Clemons TE, Davis MD, Ferris III FL, Gensler GR, Kurinij N, Lindblad AS, Milton RC, Seddon JM, Sperduto RD. Age-Related Eye Disease Study Research Group, The

- relationship of dietary lipid intake and age-related macular degeneration in a case-control study: AREDS Report No. 20. *Arch. Ophthalmol.* 2007; 125:671–679. [PubMed: 17502507]
7. Wymann MP, Schneider R. Lipid signalling in disease. *Nat. Rev. Mol. Cell Biol.* 2008; 9:162–176. [PubMed: 18216772]
 8. Serhan CN, Chiang N, Van Dyke TE. Resolving inflammation: Dual anti-inflammatory and pro-resolution lipid mediators. *Nat. Rev. Immunol.* 2008; 8:349–361. [PubMed: 18437155]
 9. Schmitz G, Ecker J. The opposing effects of n-3 and n-6 fatty acids. *Prog. Lipid Res.* 2008; 47:147–155. [PubMed: 18198131]
 10. SanGiovanni JP, Chew EY. The role of ω -3 long-chain polyunsaturated fatty acids in health and disease of the retina. *Prog. Retin. Eye Res.* 2005; 24:87–138. [PubMed: 1555528]
 11. Hardy P, Beauchamp M, Sennlaub F, Gobeil F Jr, Tremblay L, Mwaikambo B, Lachapelle P, Chemtob S. New insights into the retinal circulation: Inflammatory lipid mediators in ischemic retinopathy. *Prostaglandins Leukot. Essent. Fatty Acids.* 2005; 72:301–325. [PubMed: 15850712]
 12. Gronert K. Lipid autacoids in inflammation and injury responses: A matter of privilege. *Mol. Interv.* 2008; 8:28–35. [PubMed: 18332482]
 13. Majos A, Wolak T, Bogorodzki P, Tybor K, Sapieha M, Stefańczyk L. A blood pool contrast aided T1 functional MRI in patients with brain tumors—a preliminary study. *Neuroradiology.* 2010
 14. Funk CD. Prostaglandins and leukotrienes: Advances in eicosanoid biology. *Science.* 2001; 294:1871–1875. [PubMed: 11729303]
 15. Serhan CN. Resolution phase of inflammation: Novel endogenous anti-inflammatory and proresolving lipid mediators and pathways. *Annu. Rev. Immunol.* 2007; 25:101–137. [PubMed: 17090225]
 16. Connor KM, Krah NM, Dennison RJ, Aderman CM, Chen J, Guerin KI, Sapieha P, Stahl A, Willett KL, Smith LE. Quantification of oxygen-induced retinopathy in the mouse: A model of vessel loss, vessel regrowth and pathological angiogenesis. *Nat. Protoc.* 2009; 4:1565–1573. [PubMed: 19816419]
 17. Stahl A, Connor KM, Sapieha P, Willett KL, Krah NM, Dennison RJ, Chen J, Guerin KI, Smith LE. Computer-aided quantification of retinal neovascularization. *Angiogenesis.* 2009; 12:297–301. [PubMed: 19757106]
 18. Kang JX, Wang J, Wu L, Kang ZB. Transgenic mice: *Fat-1* mice convert *n*-6 to *n*-3 fatty acids. *Nature.* 2004; 427:504. [PubMed: 14765186]
 19. Serhan CN. Lipoxins and aspirin-triggered 15-epi-lipoxins are the first lipid mediators of endogenous anti-inflammation and resolution. *Prostaglandins Leukot. Essent. Fatty Acids.* 2005; 73:141–162. [PubMed: 16005201]
 20. Murphy RC, Gijón MA. Biosynthesis and metabolism of leukotrienes. *Biochem. J.* 2007; 405:379–395. [PubMed: 17623009]
 21. Austen KF. The mast cell and the cysteinyl leukotrienes. *Novartis Found. Symp.* 2005; 271:166–175. [PubMed: 16605134]
 22. Letts LG. Leukotrienes: Role in cardiovascular physiology. *Cardiovasc. Clin.* 1987; 18:101–113. [PubMed: 3038323]
 23. Osher E, Weisinger G, Limor R, Tordjman K, Stern N. The 5 lipoxygenase system in the vasculature: Emerging role in health and disease. *Mol. Cell. Endocrinol.* 2006; 252:201–206. [PubMed: 16647809]
 24. Peters-Golden M, Henderson WR Jr. Leukotrienes. *N. Engl. J. Med.* 2007; 357:1841–1854. [PubMed: 17978293]
 25. Murphy RC, Barkley RM, Zemski Berry K, Hankin J, Harrison K, Johnson C, Krank J, McAnoy A, Uhlson C, Zarini S. Electrospray ionization and tandem mass spectrometry of eicosanoids. *Anal. Biochem.* 2005; 346:1–42. [PubMed: 15961057]
 26. González-Pérez A, Horrillo R, Ferré N, Gronert K, Dong B, Morán-Salvador E, Titos E, Martínez-Clemente M, López-Parra M, Arroyo V, Clària J. Obesity-induced insulin resistance and hepatic steatosis are alleviated by ω -3 fatty acids: A role for resolvins and protectins. *FASEB J.* 2009; 23:1946–1957. [PubMed: 19211925]
 27. Hassan IR, Gronert K. Acute changes in dietary ω -3 and ω -6 polyunsaturated fatty acids have a pronounced impact on survival following ischemic renal injury and formation of renoprotective

- docosahexaenoic acid-derived protectin D1. *J. Immunol.* 2009; 182:3223–3232. [PubMed: 19234220]
28. Serhan CN, Lu Y, Hong S, Yang R. Mediator lipidomics: Search algorithms for eicosanoids, resolvins, and protectins. *Methods Enzymol.* 2007; 432:275–317. [PubMed: 17954222]
 29. Diau GY, Hsieh AT, Sarkadi-Nagy EA, Wijendran V, Nathanielsz PW, Brenna JT. The influence of long chain polyunsaturate supplementation on docosahexaenoic acid and arachidonic acid in baboon neonate central nervous system. *BMC Med.* 2005; 3:11. [PubMed: 15975147]
 30. Yli-Jama P, Meyer HE, Ringstad J, Pedersen JI. Serum free fatty acid pattern and risk of myocardial infarction: A case-control study. *J. Intern. Med.* 2002; 251:19–28. [PubMed: 11851861]
 31. Itoh T, Fairall L, Amin K, Inaba Y, Szanto A, Balint BL, Nagy L, Yamamoto K, Schwabe JW. Structural basis for the activation of PPAR γ by oxidized fatty acids. *Nat. Struct. Mol. Biol.* 2008; 15:924–931. [PubMed: 19172745]
 32. González-Pérez A, Planagumà A, Gronert K, Miquel R, López-Parra M, Titos E, Horrillo R, Ferré N, Deulofeu R, Arroyo V, Rodés J, Clària J. Docosahexaenoic acid (DHA) blunts liver injury by conversion to protective lipid mediators: Protectin D1 and 17S-hydroxy-DHA. *FASEB J.* 2006; 20:2537–2539. [PubMed: 17056761]
 33. Itoh T, Yamamoto K. Peroxisome proliferator activated receptor γ and oxidized docosahexaenoic acids as new class of ligand. *Naunyn Schmiedebergs Arch. Pharmacol.* 2008; 377:541–547. [PubMed: 18193404]
 34. Stahl A, Paschek L, Martin G, Gross NJ, Feltgen N, Hansen LL, Agostini HT. Rapamycin reduces VEGF expression in retinal pigment epithelium (RPE) and inhibits RPE-induced sprouting angiogenesis in vitro. *FEBS Lett.* 2008; 582:3097–3102. [PubMed: 18703055]
 35. Sapieha P, Sirinyan M, Hamel D, Zaniolo K, Joyal JS, Cho JH, Honoré JC, Kermorvant-Duchemin E, Varma DR, Tremblay S, Leduc M, Rihakova L, Hardy P, Klein WH, Mu X, Mamer O, Lachapelle P, Di Polo A, Beauséjour C, Andelfinger G, Mitchell G, Sennlaub F, Chemtob S. The succinate receptor GPR91 in neurons has a major role in retinal angiogenesis. *Nat. Med.* 2008; 14:1067–1076. [PubMed: 18836459]
 36. Holman RT. The slow discovery of the importance of ω 3 essential fatty acids in human health. *J. Nutr.* 1998; 128:427S–433S. [PubMed: 9478042]
 37. Serhan CN, Hamberg M, Samuelsson B. Lipoxins: Novel series of biologically active compounds formed from arachidonic acid in human leukocytes. *Proc. Natl. Acad. Sci. U.S.A.* 1984; 81:5335–5339. [PubMed: 6089195]
 38. Tjonahen E, Oh SF, Siegelman J, Elangovan S, Percarpio KB, Hong S, Arita M, Serhan CN. Resolvin E2: Identification and anti-inflammatory actions: Pivotal role of human 5-lipoxygenase in resolvin E series biosynthesis. *Chem. Biol.* 2006; 13:1193–1202. [PubMed: 17114001]
 39. Bazan NG. Cellular and molecular events mediated by docosahexaenoic acid-derived neuroprotectin D1 signaling in photoreceptor cell survival and brain protection. *Prostaglandins Leukot. Essent. Fatty Acids.* 2009; 81:205–211. [PubMed: 19520558]
 40. Bazan NG. Neuroprotectin D1-mediated anti-inflammatory and survival signaling in stroke, retinal degenerations, and Alzheimer's disease. *J. Lipid Res.* 2009; 50(Suppl):S400–S405. [PubMed: 19018037]
 41. Lehmann JM, Moore LB, Smith-Oliver TA, Wilkison WO, Willson TM, Kliewer SA. An antidiabetic thiazolidinedione is a high affinity ligand for peroxisome proliferator-activated receptor γ (PPAR γ). *J. Biol. Chem.* 1995; 270:12953–12956. [PubMed: 7768881]
 42. Altiock S, Xu M, Spiegelman BM. PPAR γ induces cell cycle withdrawal: Inhibition of E2F/DP DNA-binding activity via down-regulation of PP2A. *Genes Dev.* 1997; 11:1987–1998. [PubMed: 9271121]
 43. Murata T, Hata Y, Ishibashi T, Kim S, Hsueh WA, Law RE, Hinton DR. Response of experimental retinal neovascularization to thiazolidinediones. *Arch. Ophthalmol.* 2001; 119:709–717. [PubMed: 11346398]
 44. Shen LQ, Child A, Weber GM, Folkman J, Aiello LP. Rosiglitazone and delayed onset of proliferative diabetic retinopathy. *Arch. Ophthalmol.* 2008; 126:793–799. [PubMed: 18541841]

45. Graham DJ, Ouellet-Hellstrom R, MaCurdy TE, Ali F, Sholley C, Worrall C, Kelman JA. Risk of acute myocardial infarction, stroke, heart failure, and death in elderly Medicare patients treated with rosiglitazone or pioglitazone. *JAMA*. 2010; 304:411–418. [PubMed: 20584880]
46. Lee JH, O'Keefe JH, Lavie CJ, Harris WS. Omega-3 fatty acids: Cardiovascular benefits, sources and sustainability. *Nat. Rev. Cardiol*. 2009; 6:753–758. [PubMed: 19859067]
47. Smith LE, Wesolowski E, McLellan A, Kostyk SK, D'Amato R, Sullivan R, D'Amore PA. Oxygen-induced retinopathy in the mouse. *Invest. Ophthalmol. Vis. Sci*. 1994; 35:101–111. [PubMed: 7507904]
48. Aiello LP, Pierce EA, Foley ED, Takagi H, Chen H, Riddle L, Ferrara N, King GL, Smith LE. Suppression of retinal neovascularization in vivo by inhibition of vascular endothelial growth factor (VEGF) using soluble VEGF-receptor chimeric proteins. *Proc. Natl. Acad. Sci. U.S.A*. 1995; 92:10457–10461. [PubMed: 7479819]
49. Robinson GS, Pierce EA, Rook SL, Foley E, Webb R, Smith LE. Oligodeoxynucleotides inhibit retinal neovascularization in a murine model of proliferative retinopathy. *Proc. Natl. Acad. Sci. U.S.A*. 1996; 93:4851–4856. [PubMed: 8643492]
50. Adamis AP, Shima DT, Tolentino MJ, Gragoudas ES, Ferrara N, Folkman J, D'Amore PA, Miller JW. Inhibition of vascular endothelial growth factor prevents retinal ischemia-associated iris neovascularization in a nonhuman primate. *Arch. Ophthalmol*. 1996; 114:66–71. [PubMed: 8540853]
51. Stahl A, Connor KM, Sapieha P, Chen J, Dennison RJ, Krah NM, Seaward MR, Willett KL, Aderman CM, Guerin KI, Hua J, Löfqvist C, Hellström A, Smith LE. The mouse retina as an angiogenesis model. *Invest. Ophthalmol. Vis. Sci*. 2010; 51:2813–2826. [PubMed: 20484600]
52. Serhan CN, Clish CB, Brannon J, Colgan SP, Chiang N, Gronert K. Novel functional sets of lipid-derived mediators with antiinflammatory actions generated from ω -3 fatty acids via cyclooxygenase 2-nonsteroidal antiinflammatory drugs and transcellular processing. *J. Exp. Med*. 2000; 192:1197–1204. [PubMed: 11034610]
53. Serhan CN, Levy BD, Clish CB, Gronert K, Chiang N. Lipoxins, aspirin-triggered 15-epi-lipoxin stable analogs and their receptors in anti-inflammation: A window for therapeutic opportunity. *Ernst Schering Res. Found. Workshop*. 2000:143–185. [PubMed: 10943332]
54. Serhan CN, Hong S, Gronert K, Colgan SP, Devchand PR, Mirick G, Moussignac RL. Resolvins: A family of bioactive products of ω -3 fatty acid transformation circuits initiated by aspirin treatment that counter proinflammation signals. *J. Exp. Med*. 2002; 196:1025–1037. [PubMed: 12391014]
55. Hong S, Gronert K, Devchand PR, Moussignac RL, Serhan CN. Novel docosatrienes and 17*S*-resolvins generated from docosahexaenoic acid in murine brain, human blood, and glial cells. Autacoids in anti-inflammation. *J. Biol. Chem*. 2003; 278:14677–14687. [PubMed: 12590139]
56. Kanaoka Y, Maekawa A, Penrose JF, Austen KF, Lam BK. Attenuated zymosan-induced peritoneal vascular permeability and IgE-dependent passive cutaneous anaphylaxis in mice lacking leukotriene C4 synthase. *J. Biol. Chem*. 2001; 276:22608–22613. [PubMed: 11319240]
57. Serhan CN, Savill J. Resolution of inflammation: The beginning programs the end. *Nat. Immunol*. 2005; 6:1191–1197. [PubMed: 16369558]
58. Moriguchi T, Lim SY, Greiner R, Lefkowitz W, Loewke J, Hoshiba J, Salem N Jr. Effects of an n-3-deficient diet on brain, retina, and liver fatty acyl composition in artificially reared rats. *J. Lipid Res*. 2004; 45:1437–1445. [PubMed: 15175358]
59. Leesnitzer LM, Parks DJ, Bledsoe RK, Cobb JE, Collins JL, Consler TG, Davis RG, Hull-Ryde EA, Lenhard JM, Patel L, Plunket KD, Shenk JL, Stimmel JB, Therapontos C, Willson TM, Blanchard SG. Functional consequences of cysteine modification in the ligand binding sites of peroxisome proliferator activated receptors by GW9662. *Biochemistry*. 2002; 41:6640–6650. [PubMed: 12022867]
60. Liu D, Zeng BX, Zhang SH, Yao SL. Rosiglitazone, an agonist of peroxisome proliferator-activated receptor γ reduces pulmonary inflammatory response in a rat model of endotoxemia. *Inflamm. Res*. 2005; 54:464–470. [PubMed: 16307220]
61. Gronert K, Clish CB, Romano M, Serhan CN. Transcellular regulation of eicosanoid biosynthesis. *Methods Mol. Biol*. 1999; 120:119–144. [PubMed: 10343315]

62. Brault S, Gobeil F Jr, Fortier A, Honoré JC, Joyal JS, Sapieha PS, Kooli A, Martin E, Hardy P, Ribeiro-da-Silva A, Peri K, Lachapelle P, Varma D, Chemtob S. Lysophosphatidic acid induces endothelial cell death by modulating the redox environment. *Am. J. Physiol. Regul. Integr. Comp. Physiol.* 2007; 292:R1174–R1183. [PubMed: 17122328]
63. Korff T, Augustin HG. Integration of endothelial cells in multicellular spheroids prevents apoptosis and induces differentiation. *J. Cell Biol.* 1998; 143:1341–1352. [PubMed: 9832561]

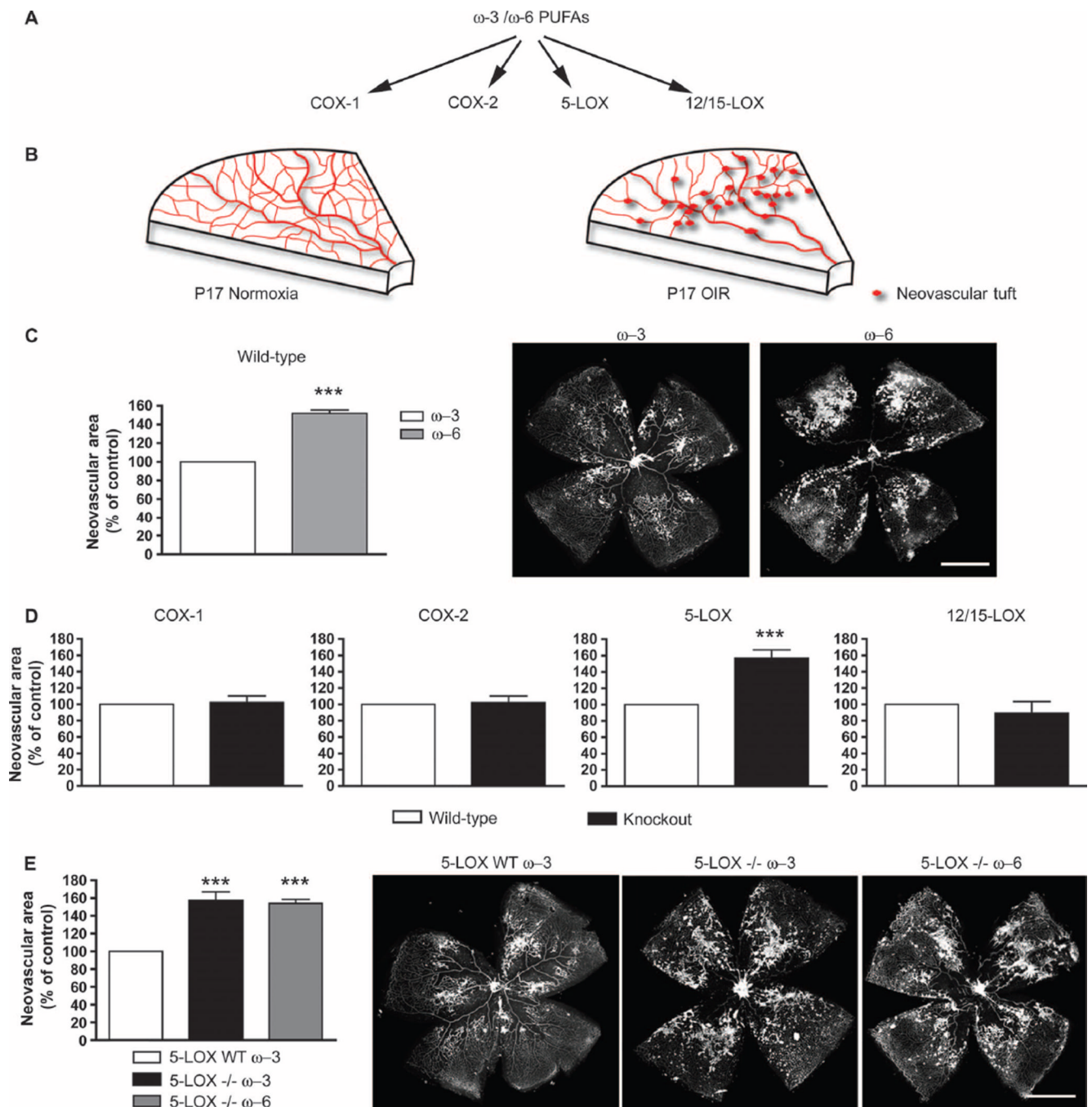


Fig. 1. 5-Lipoxygenase (5-LOX) mediates ω -3 PUFA suppression of neo-vascularization in oxygen-induced retinopathy (OIR). (A) Schematic of major ω -3 and ω -6 PUFA metabolism pathways. (B) Graphic depiction of vascular phenotypes from normoxic and OIR P17 mouse retinas. (C) Neovascularization at P17 in retinas of wild-type (WT) mice with OIR fed either ω -3 ($n = 24$) or ω -6 ($n = 14$) PUFAs from birth. Representative images of retinal flat mounts are displayed. (D) Quantified neovascularization in ω -3 PUFA-fed $COX-1^{-/-}$ ($n = 16$), $COX-2^{-/-}$ ($n = 24$), $5-LOX^{-/-}$ ($n = 24$), and $12/15-LOX^{-/-}$ ($n = 12$) mice compared to their respective ω -3 PUFA-fed WT controls at P17. (E) Quantification of

neovascularization at P17 in *5-LOX* WT mice fed ω -3 PUFAs compared to *5-LOX*^{-/-} mice fed either ω -3 or ω -6 PUFAs ($n = 24$ for all groups). n signifies number of eyes quantified. Representative images of retinal flat-mounts from each data set are shown. All values are percentage of neovascularization area over total retinal area and are expressed as a percentage of mean neovascularization in each strain-specific WT group; for absolute values, see fig. S1. Scale bars, 500 μ m. *** $P < 0.0001$.

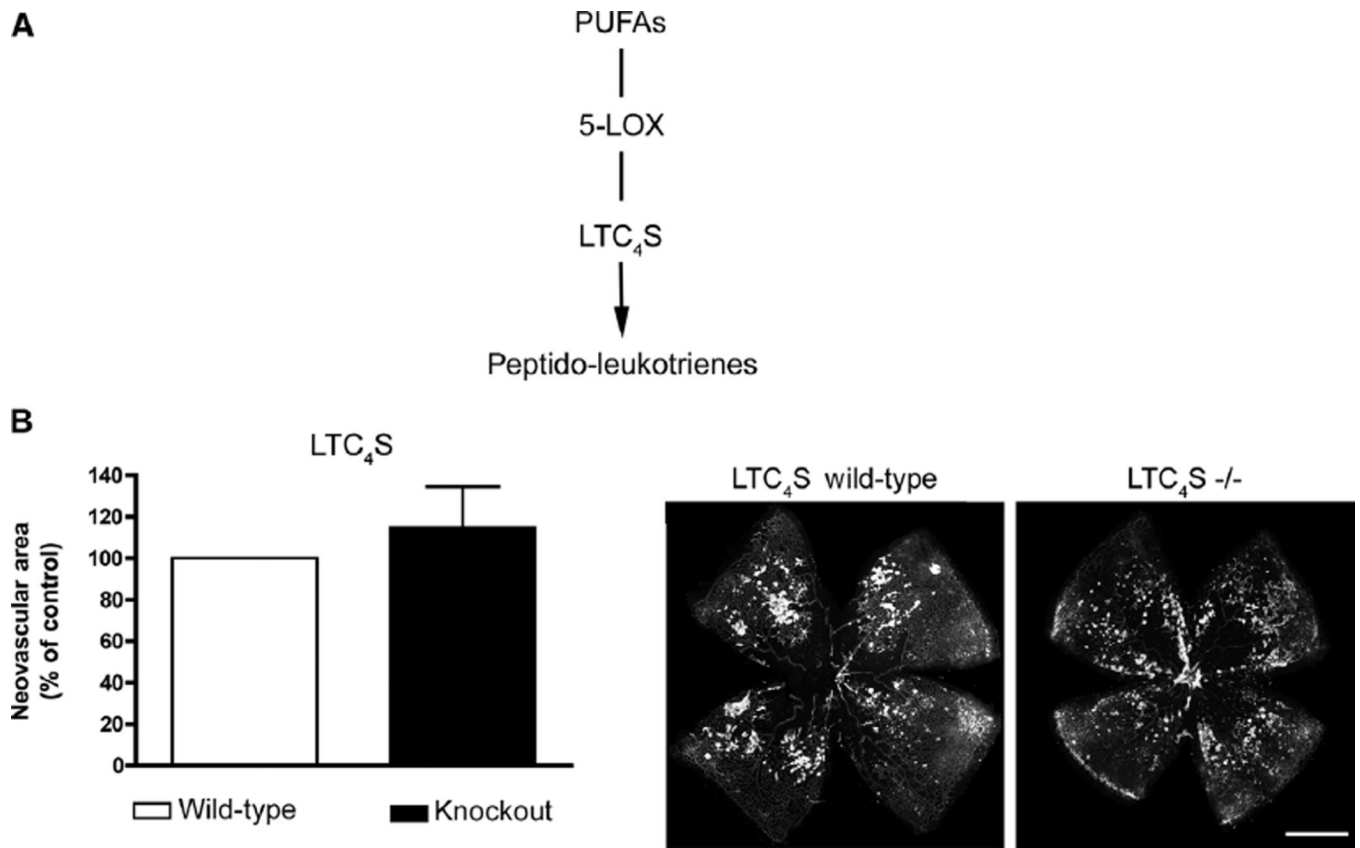


Fig. 2. The cysteinyl-leukotriene pathway does not contribute to the protective effects of 5-LOX on retinopathy. **(A)** Schematic of production of peptido-leukotrienes by 5-LOX. **(B)** Quantification of retinal neovascularization at P17 in *LTC₄S*^{-/-} and WT control mice fed ω -3-rich diets and subjected to OIR ($P = 0.0929$; $n = 26$). Representative images are shown. Scale bar, 500 μ m.

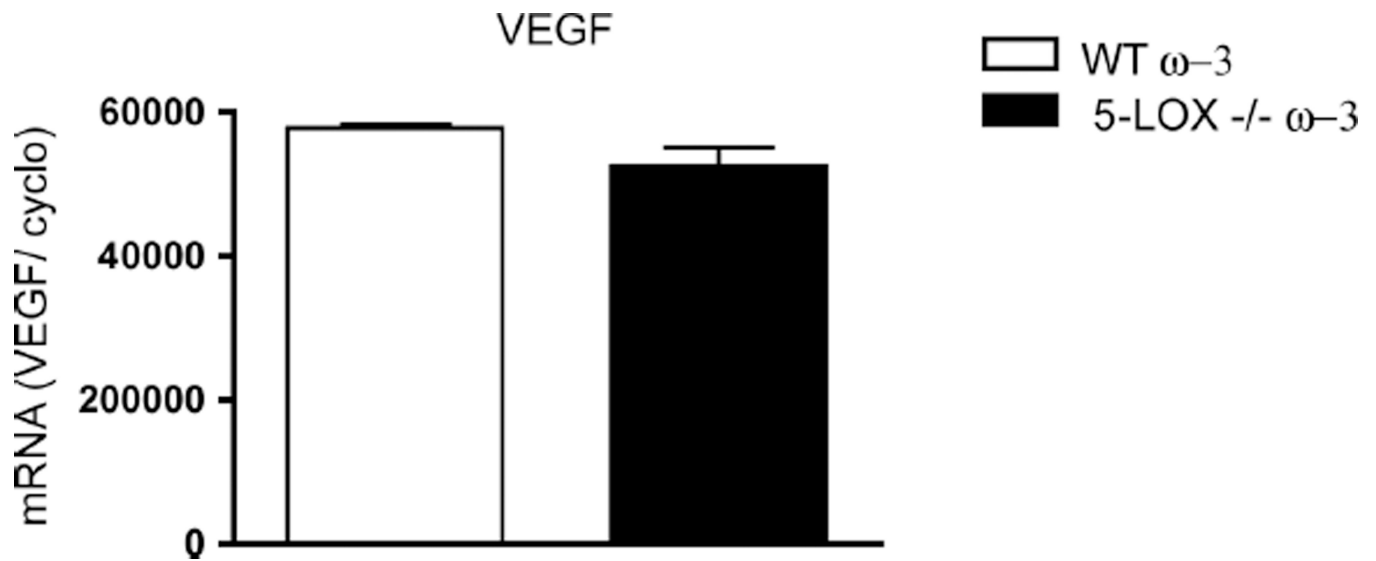


Fig. 3. VEGF levels in 5-LOX^{-/-} mice remain unaffected. Real-time PCR analysis and quantification of VEGF mRNA reveal no change in expression at P17H expression in ω -3 PUFA-fed WT and 5-LOX^{-/-} whole retinas, normalized to millions of copies of *CyclophilinA* mRNA ($P = 0.1236$; $n = 3$).

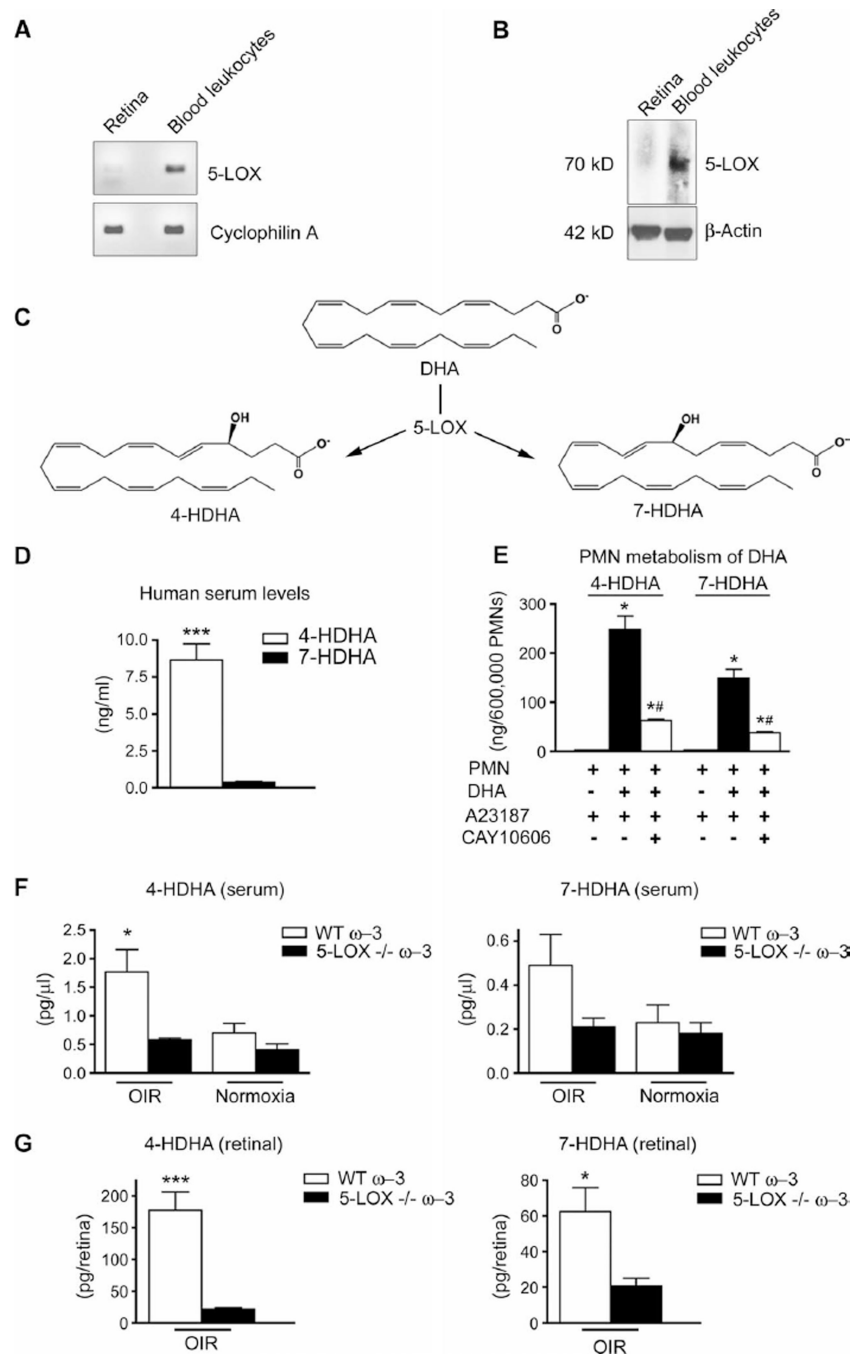


Fig. 4. The leukocyte-derived 5-LOX metabolites 4-HDHA and 7-HDHA are enriched in serum and retina during OIR. **(A)** PCR analysis of *5-LOX* mRNA from whole retina and blood leukocytes normalized to millions of copies of *CyclophilinA* mRNA ($n = 3$). **(B)** Western blot analysis of 5-LOX protein from whole retina and blood leukocytes ($n = 3$) reveals an immunoreactive band at ~75 kD. **(C)** Schematic depicting metabolism of DHA through 5-LOX into 4-HDHA and 7-HDHA. **(D)** 4-HDHA and 7-HDHA in human serum from healthy male subjects ($n = 28$) in a model of physiologically activated leukocytes (blood clotting). **(E)** 5-LOX-specific formation of 4-HDHA and 7-HDHA by mouse polymorphonuclear

leukocytes (PMNs) after activation with a calcium ionophore (A23187; 2 μM) in presence or absence of DHA (10 μM), with or without a specific 5-LOX-reversible inhibitor (CAY10606; 50 μM) ($n = 4$). **(F)** Systemic serum concentrations of 4-HDHA ($n = 5$) and 7-HDHA ($n = 6$) in WT and 5-LOX^{-/-} mice with OIR and in normoxic mice at P17. **(G)** Retinal concentrations of 4-HDHA ($n = 6$) and 7-HDHA ($n = 4$) in OIR WT and 5-LOX^{-/-} mice. * $P < 0.05$; ** $P < 0.001$; *** $P < 0.0005$; # $P < 0.05$ versus PMN + DHA + A23187.

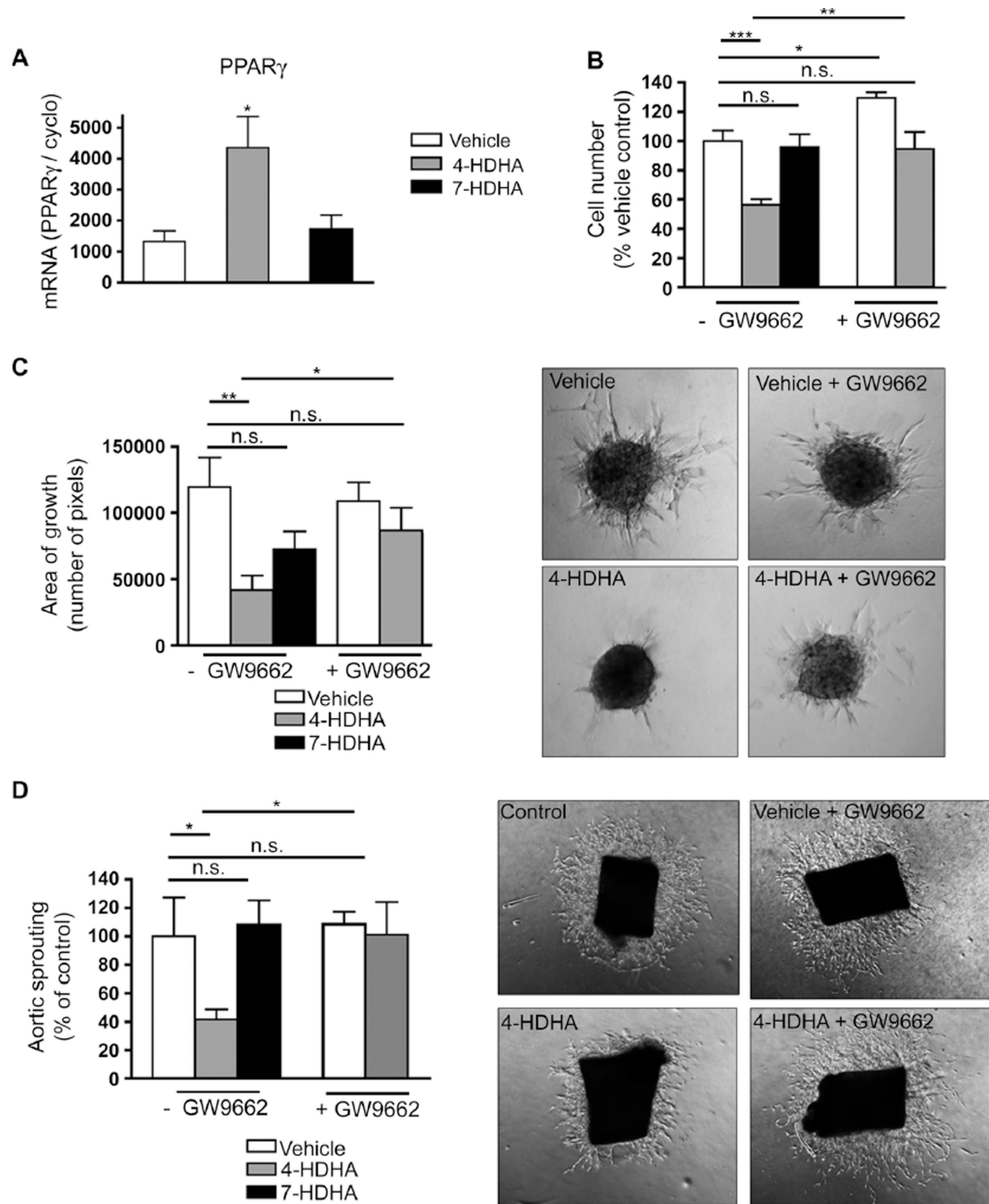


Fig. 5. 4-HDHA directly modulates endothelial cell proliferation and vascular sprouting through activation of PPAR γ (A) qPCR quantification of *PPAR\gamma* mRNA of cultured HRECs treated with 4-HDHA or 7-HDHA; all groups were normalized to millions of copies of *CyclophilinA* mRNA ($n = 3$). (B) Proliferation of HRECs treated with vehicle ($n = 5$), 4-HDHA (3 μ M) ($n = 10$), or 7-HDHA (3 μ M) ($n = 9$) with or without GW9662 (3 μ M) present ($n = 5$). (C) Spheroid assay of microvascular sprouting: retinal endothelial cells treated with vehicle ($n = 9$), 4-HDHA ($n = 10$), or 7-HDHA ($n = 17$) in the presence and absence of GW9662 (3 μ M) ($n = 11$); sprouting was quantified 24 hours after treatment. (D)

Aortic ring assay of microvascular sprouting: Aortic rings were treated with vehicle, 4-HDHA, or 7-HDHA in the presence and absence of GW9662 (3 μ M). Area of sprouting was quantified 48 hours after treatment ($n = 5$). For (C) and (D), images representative of the quantification are shown at the right. * $P < 0.05$; ** $P < 0.005$; *** $P < 0.0001$.

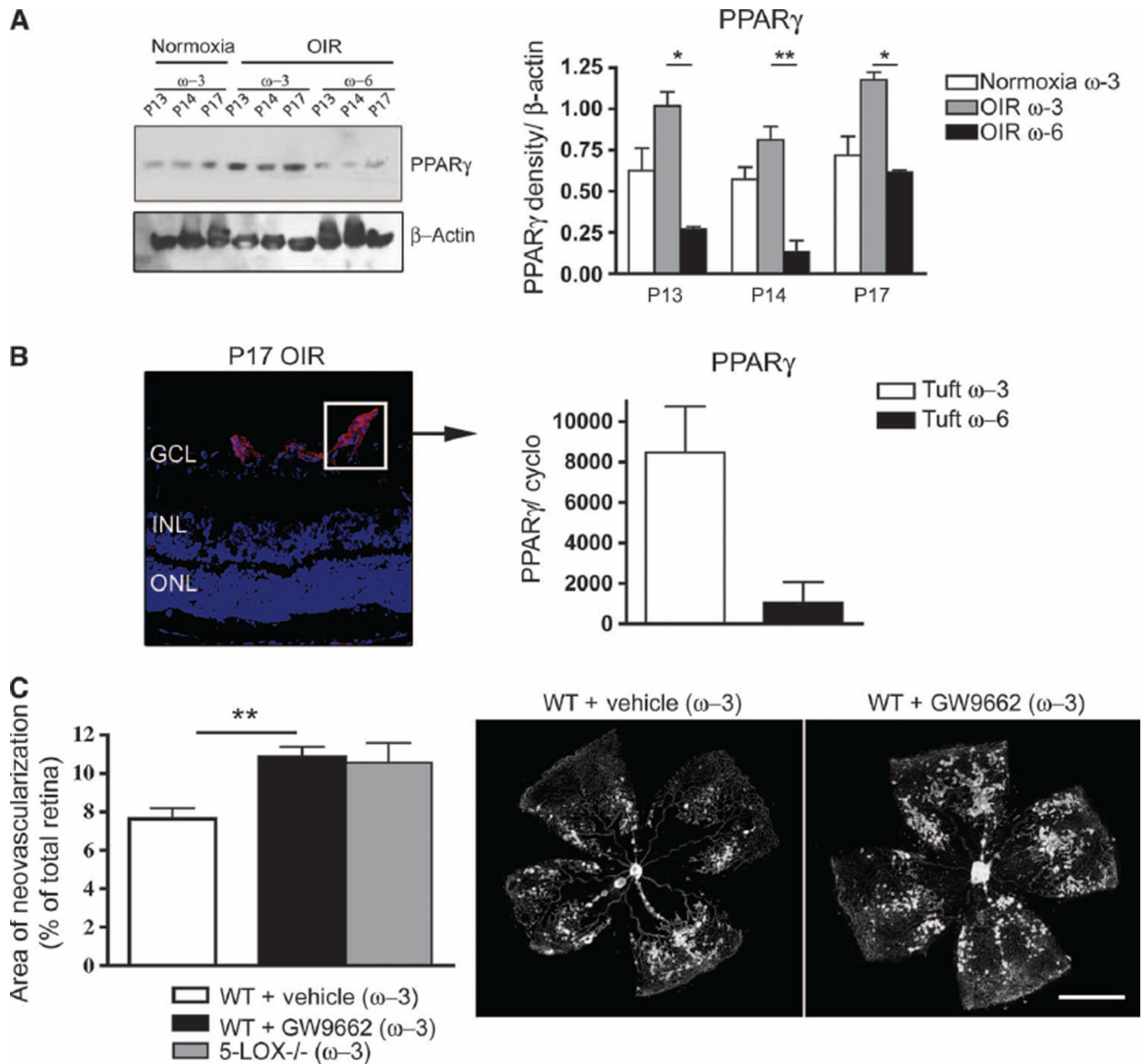


Fig. 6. ω -3 PUFAs induce neovessel-specific expression of *PPAR γ* , which mediates the antiangiogenic effects of ω -3 PUFAs in retinopathy. **(A)** Western blot and densitometry analysis for *PPAR γ* in P13, P14, and P17 retinas from ω -3 PUFA-fed normoxic mice and mice with OIR fed either ω -3 or ω -6 PUFA diets. **(B)** qPCR quantification of *PPAR γ* mRNA from laser-captured tufts (pathological neovessels) (at P17), normalized to a million copies of *CyclophilinA* mRNA. Left-hand panel indicates a tuft (neovessel sprout) representative of the captured cell population. **(C)** Quantification of neovascularization at P17 in ω -3 PUFA-fed WT mice injected with vehicle or GW9662 (3 μ M) ($n = 6$) and ω -3-fed *5-LOX*^{-/-} mice. Scale bar, 500 μ m. * $P < 0.05$; ** $P < 0.005$.